PRAMANA — journal of physics

Vol. 80, No. 5
May 2013
pp. 887–894

Nonlinear properties of a graded-index photonic heterostructure

B TAVAKKOLY MOGHADDAM[1], S ROSHAN ENTEZAR[2,*] and H PASHAEI ADL[2]

[1]Shabestar Branch, Islamic Azad University, Shabestar, Iran
[2]Faculty of Physics, Bahman, University of Tabriz, Tabriz, BoBox: 5167618949, Iran
*Corresponding author. E-mail: s-roshan@tabrizu.ac.ir

MS received 1 February 2012; revised 26 November 2012; accepted 6 December 2012

Abstract. The optical properties of a one-dimensional (1D) photonic heterostructure with graded-index nonlinear materials are demonstrated theoretically. The influence of the gradation profile of the graded-index nonlinear layers on the linear and nonlinear responses of the structure are analysed. It is shown that the Q-factor of the defect mode and the threshold input intensity to achieve the optical bistability in the used photonic heterostructure depend on the gradation profile of the graded-index nonlinear layers.

Keywords. Photonic heterostructure; graded index; nonlinear materials; optical bistability.

PACS Nos 42.70.Qs; 42.65.Pc; 42.79.Ry; 42.25.Bs

1. Introduction

Photonic crystals (PCs), which exhibit photonic band structures due to multiple Bragg scattering, have attracted considerable attention in recent years because of their electromagnetic properties and their important potential applications [1–4]. They are classified into three categories: one-dimensional (1D), two-dimensional (2D), and three-dimensional (3D) crystals in terms of the dimensionality of stacks [5]. PCs that work in the microwave and the far-infrared regions are relatively easy to fabricate. However, PCs for the visible and the infrared regions, especially, 3D PCs, are difficult to fabricate because of their small lattice constant, which must be comparable to the wavelength [6]. Therefore, 1D PCs, which can be produced easily by thin-film deposition techniques, are preferable for use in the visible and IR regions [7]. Furthermore, light can be manipulated by introducing defects into the 1D PCs. The defect modes lead to the selective transmission in the 1D PCs and make studies on 1D PCs even more attractive [8,9].

Optical bistability (OB) is another important way to control the propagation of photons [10–12]. In the presence of nonlinear defect modes, the OB can be produced by the

dynamic shifting of defect modes [13,14]. Inouyea and Kanemitsu directly observed the shifting of defect mode in experiment and opened the fields for applying PCs with defects to the nonlinear optical devices [15]. The basic way to reduce OB threshold significantly is to search for a nonlinear defect with proper physical parameters or increase the number of nonlinear layers [16,17]. However, selecting an appropriate Kerr material is very difficult and too much thickness is disadvantageous for 1D nonlinear photonic crystal devices. New methods to reduce the OB threshold intensity are expected. To achieve suitable defect modes, efforts are on to obtain tunability of the position and intensity of the defect modes [18,19].

Recently, studies were conducted on the graded-index materials as one of the advanced heterogeneous composite materials in various engineering applications [20,21]. The graded-index materials are materials for which the optical properties can vary continuously in space. The change in the physical properties makes the graded-index materials to behave very differently from the homogeneous materials and conventional composite materials. In this paper, a new method is presented to control the OB behaviour of PCs. We introduce a 1D photonic heterostructure containing nonlinear graded-index materials. This composite structure can exhibit a bistability that can be strongly modulated by the gradation profile of the graded-index layers. We can realize very low OB threshold values just by carefully choosing the gradation profile of the graded-index layers, instead of adjusting the nonlinear materials or increasing the number of layers.

2. Theoretical model

We consider the symmetric quarter-wavelength stack $(BA)^m(AB)^m$ or $(AB)^m(BA)^m$ as our 1D photonic heterostructure, where m is the period number. The constituent layers A and B are considered to be linear nongraded and nonlinear graded-index dielectric materials, respectively. Thicknesses of the two types of layers are such that

$$n_A d_a = \int_0^{d_B} n_B(z)\mathrm{d}z = \lambda_0/4, \tag{1}$$

where $\lambda_0 = 550$ nm is the midgap wavelength. So, the total optical thickness of the sample is $m\lambda_0$. This type of structure can create a defect mode with frequency $\omega_0 = 2\pi c/\lambda_0$ in the middle of the band gap. Without loss of generality, the surrounding environment is assumed to be vacuum. We choose a coordinate system in which the layers have normal vector along z-axis and assume that $\varepsilon_A = 4$ and $\varepsilon_B = \varepsilon(z) + \alpha|E(z)|^2$. Here, $\varepsilon(z)$ is the linear dielectric permittivity of the graded-index layer B which varies along the direction perpendicular to the surface of the layers. $E(z)$ is the local electric field in the nonlinear graded-index layers and α is the nonlinear coefficient. For the linear electric permittivity of the graded-index layer B, we consider five different gradation profiles as

$$\begin{aligned}
&(1)\quad \varepsilon(\xi) = 4\mathrm{e}^{-0.5\xi},\\
&(2)\quad \varepsilon(\xi) = 2.25 + 1.75(2\xi - 1)^2,\\
&(3)\quad \varepsilon(\xi) = 4\mathrm{e}^{-0.5(2\xi-1)^2},\\
&(4)\quad \varepsilon(\xi) = 2.25 + 1.75\xi,\\
&(5)\quad \varepsilon(\xi) = 2.75\mathrm{e}^{0.375(2\xi-1)^2},
\end{aligned} \tag{2}$$

and compare our results with the nongraded profile

$$(6)\quad \varepsilon(\xi) = 3.125,$$

where $\xi = z/d_B$. In the above gradation profiles, the numerical parameters are selected so that the optical path length of the layer B is $\lambda_0/4$. Figure 1 shows schematically the 1D photonic heterostructure $(AB)^m(BA)^m$ with such gradation profiles. Here, we see that the profiles 2 and 5 do not have abrupt changes in their permittivities (see figures 1b and 1e), whereas, all the other profiles have at least one abrupt change from its maximum value to its minimum value or vice versa. An z-dependent profile for the relative permittivity can be achieved experimentally by imposing a temperature profile or doping methods [22,23].

Consider a monochromatic TE-polarized plane wave incident from air at an angle θ with the normal to the surface of the 1D heterostructure (i.e. the z-axis). The tangential (to the interfaces) components of the electric fields across the lth layer of width d_l are related by the following transfer matrix [24]:

$$M_l = \begin{pmatrix} \cos k_{zl} d_l & (i\omega/ck_{zl}) \sin k_{zl} d_l \\ (ck_{zl}/i\omega) \sin k_{zl} d_l & \cos k_{zl} d_l \end{pmatrix}, \tag{3}$$

where $k_{zl} = (\omega/c)\sqrt{\varepsilon_l - \sin^2\theta}$. Therefore, the incident field can be related to the transmitted field of the linear multilayered structure by using the transfer matrix M_l. It is known that for the linear multilayered structure, we can investigate the transmission properties using the transfer-matrix method. Based on the fact that an arbitrary gradation profile can be approached by a series of piecewise profiles, the graded-index layers can be divided into a number of sublayers and each sublayer is assumed to be homogeneous. Hence, we can use transfer matrix method [25,26] to obtain the linear properties of the structure. However, in nonlinear case, the dielectric property in nonlinear layers will be dependent on the local field intensity. In the nonlinear case, one can use the nonlinear transfer matrix [27] approach to calculate the transmission coefficient of the structure. In

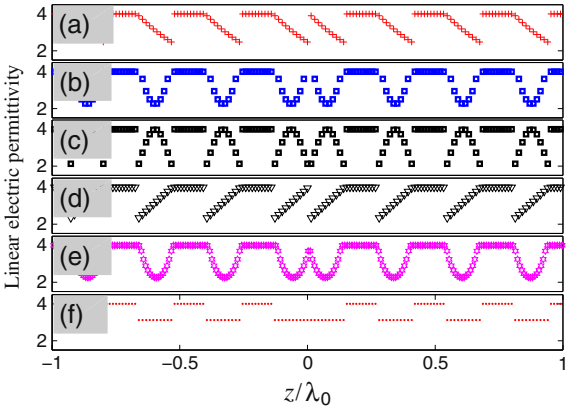

Figure 1. Sketch of a typical 1D photonic heterostructure $(AB)^m(BA)^m$, with (**a**) $\varepsilon(\xi) = 4e^{-0.5\xi}$, (**b**) $\varepsilon(\xi) = 2.25 + 1.75(2\xi - 1)^2$, (**c**) $\varepsilon(\xi) = 4e^{-0.5(2\xi-1)^2}$, (**d**) $\varepsilon(\xi) = 2.25 + 1.75\xi$, (**e**) $\varepsilon(\xi) = 2.75e^{0.375(2\xi-1)^2}$ and (**f**) nongraded profile $\varepsilon(\xi) = 3.125$. Here, we considered $\varepsilon_A = 4$.

this approach, the values of k_{zl} and ε_l for the nonlinear layers are determined using the value of electric field intensity at the corresponding interfaces. The tangential components of electric and magnetic fields at the incident side $z = -L$ and at the transmitted side $z = L$ are related by the following matrix equation:

$$\begin{bmatrix} E_y \\ H_x \end{bmatrix}_{z=-L} = \left(\prod_{l=1}^{4m} M_l \right) \begin{bmatrix} E_y \\ H_x \end{bmatrix}_{z=L}, \tag{4}$$

where $L = m(d_A + d_B)$. Then, the transmission coefficient T of the finite structure is calculated in the usual manner.

3. Results and discussion

Now, we want to investigate the linear and nonlinear optical properties of the structure with different gradation profiles using the previously mentioned transfer matrix method. Based on the fact that an arbitrary gradation profile can be approached by a series of piecewise profiles, the graded-index layers can be divided into a number of sublayers and each sublayer is assumed to be homogeneous. Since gradation profiles 2, 3, 5 vary much further than the other profiles, in our simulations, we divided the graded-index layers with gradation profiles 2, 3, 5 into 100 sublayers and the others into 50 sublayers.

First of all, we investigate the linear transmission spectra of the structure with different gradation profiles. We plot the linear transmission spectra of the structures (a) $(AB)^{10}(BA)^{10}$ and (b) $(BA)^{10}(AB)^{10}$ at the normal incidence (i.e. $\theta = 0$) in figure 2. The figure reveals that the Q-factor of the defect modes appeared around the frequency ω_0 in both structures depends on the gradation profiles of the graded-index layers. Particularly, the defect mode of the structure $(BA)^{10}(AB)^{10}$ with gradation profile 1 has the highest Q-factor, while, in the structure $(AB)^{10}(BA)^{10}$ the highest Q-factor belongs to the defect mode of the gradation profile 2. As one can see from figure 1, the gradation profile 1 has an abrupt change in its permittivity, whereas, the gradation profile 2 varies continuously. So, the highest Q-factor of defect mode is only due to the proper choice of the gradation profile. Moreover, we see that the peaks of the defect modes of the

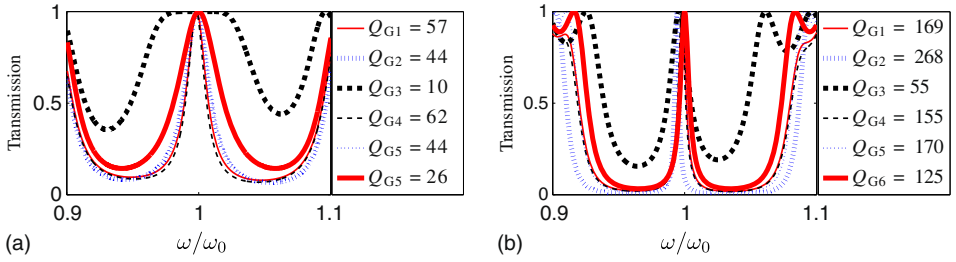

Figure 2. Linear transmission spectra of the structures (**a**) $(AB)^{10}(BA)^{10}$ and (**b**) $(BA)^{10}(AB)^{10}$ for gradation profiles 1 (thin solid line), 2 (thick dotted line), 3 (thick dashed line), 4 (thin dashed line), 5 (thin dotted line) and nongraded profile 6 (thick solid line). Here, the legends show the Q-factor of the defect modes for different gradation profiles.

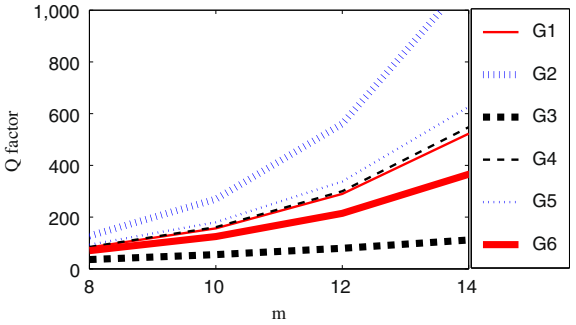

Figure 3. Q-factor of the structure $(AB)^m(BA)^m$ vs. the period number m for different gradation profiles.

graded-index structures are shifted from the mid-gap frequency ω_0. Our investigations indicate that the maximum shift from the mid-gap frequency is less than $0.007\omega_0$. Here, we assumed that the optical path length of the graded-index layers is the same for all gradation profiles. As the local wave impedance of the graded-index layers depend on the gradation profiles, it seems that the position of defect modes are affected by the wave impedance of the graded-index layers [28,29].

As Q-factors of the defect modes in the structure $(AB)^{10}(BA)^{10}$ are higher than the Q-factors of the structure $(BA)^{10}(AB)^{10}$ (see figure 2b), in what follows, we consider only the structure $(AB)^m(BA)^m$ with different gradation profiles. Then, we investigate the effect of period number m on Q-factors of the defect modes of the structure with different gradation profiles. Figure 3 represents the Q-factor of the defect modes of the structure $(AB)^m(BA)^m$ vs. the period number m for different gradation profiles. As expected, the Q-factor of the defect modes increases by increasing the period number m. However, we see that the highest Q-factor always belongs to the defect mode of the structure with the gradation profile 2.

Until now, we have considered the normal incidence case (i.e. $\theta = 0$). However, the frequency of defect mode depends on the incidence angle θ and polarization. Figure 4 shows the normalized defect mode frequency ω/ω_0 of the structure with different gradation profiles vs. incidence angle θ for both TE and TM polarizations. One can easily see that the frequency of defect modes shifts from the mid-gap frequency ω_0 towards higher

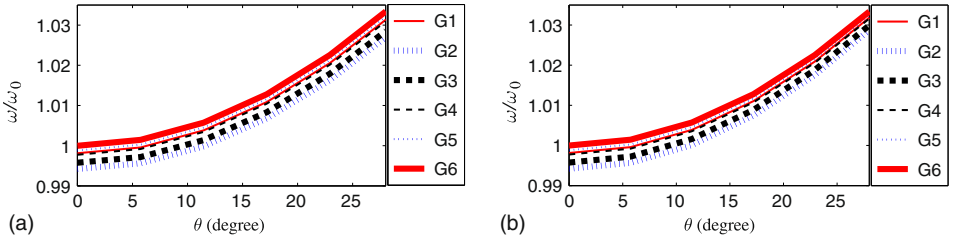

Figure 4. Normalized frequency of defect modes (ω/ω_0) vs. incidence angle θ for (**a**) TE polarization and (**b**) TM polarization.

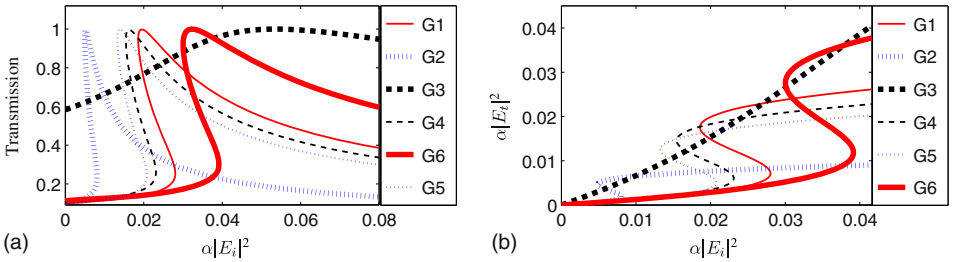

Figure 5. (**a**) Nonlinear transmission spectra and (**b**) the dimensionless output intensities $\alpha|E_t|^2$ vs. the dimensionless input control intensity $\alpha|E_i|^2$ at $\omega = 0.98\omega_0$.

frequencies. For simplicity, we consider only the normal incidence case in what follows (for which there is no difference between the TE and TM polarizations).

Then, we investigate the OB behaviour of the structure $(AB)^{10}(BA)^{10}$ near the defect mode frequency ω_0 for different gradation profiles of the graded-index nonlinear layers. Here, we assume that the permittivity of the graded-index layers is nonlinear with positive Kerr coefficient. Introducing positive Kerr coefficient leads to the OB and gap soliton formation near the low-frequency edge of the defect mode due to the enhancement of the electric field [30,31]. When Kerr coefficient is negative, OB can be seen only near the upper edge of the defect mode [32]. Although most naturally occurring materials have positive Kerr coefficient, the occurrence of negative Kerr nonlinearity in different composite crystals has been experimentally demonstrated [33–35]. However, we take the sign of the Kerr coefficient to be positive. Figures 5a and 5b show the transmittance and the dimensionless output intensity $\alpha|E_t|^2$ vs. dimensionless input intensity $\alpha|E_i|^2$ at the typical frequency $\omega = 0.98\omega_0$. The figures show bistable hysteresis loops for gradation profiles 1, 2, 4, 5 and nongraded profile 6, whereas the structure does not show any bistable behaviour for the gradation profile 3 at $\omega = 0.98\omega_0$. Here, we see that the structure with the gradation profile 2 has the lowest threshold switching intensity.

In order to have more insight about the nonlinear properties of the structure we plot the transmission spectra for the frequencies lying close to the lower edges of the defect modes

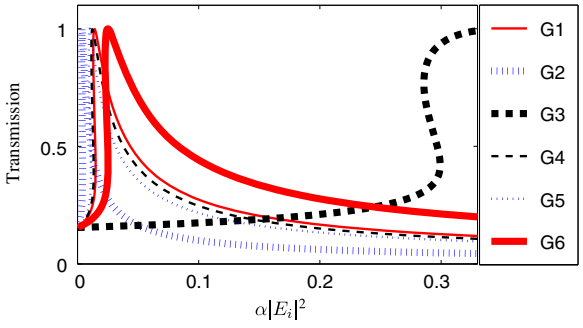

Figure 6. Nonlinear transmission spectra as a function of the dimensionless input intensity ($\alpha|E_i|^2$) at the frequencies, lying close to the lower edges of the defect modes with the linear transmission 0.15.

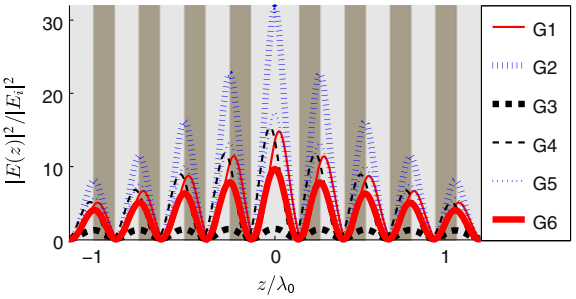

Figure 7. Electric field profiles inside the structure corresponding to the points with the nonlinear transmission 1.

with the linear transmission $T = 0.15$ in figure 6. As one can see from the figure, in this case the structure shows bistable behaviour for all gradation profiles. Although these curves have bistable behaviours, they are much different from each other. It is obvious from figure 6 that the threshold intensity needed to achieve the bistability depends on the gradation profile of the nonlinear layers. As the figure reveals, the bistable behaviour becomes prominent for the gradation profile 2 due to the lowest threshold switching intensity. In this case the nonlinear effects are magnified greatly, giving rise to optical bistability at extremely low values of input intensity. To show this, we plotted the electric field profiles inside the structure in figure 7. Here, we considered the points with the nonlinear transmission 1 from the nonlinear transmission curves in figure 6. The figure shows that the magnification of the electric field intensity significantly depends on the gradation profile. We see that the field intensity is magnified for the gradation profile 2 up to 30 times of its input value at the defect position, whereas the magnification is less than 15 for other gradation profiles. Consequently, the nonlinear effects are magnified remarkably for the gradation profile 2 giving rise to the optical bistability at the relatively low input intensity.

4. Conclusion

We have studied the linear and nonlinear responses of a 1D heterostructure with Kerr-type nonlinear graded-index layers. The linear and nonlinear behaviour of the whole system is significantly changed by the gradation profile. It is shown that by carefully choosing the gradation profiles of graded-index layers, we can realize high Q defect modes and low OB threshold values. Moreover, the results reveal that low threshold intensity and high field magnification are due to the gradation profile of graded-index nonlinear layers and not due to the presence or absence of abrupt change in permittivity.

Acknowledgement

The authors are grateful for the financial support from Shabestar Branch of Islamic Azad University (Shabester, Iran) (Grant No. 51953900330002).

References

[1] M Bayindir, B Temelkuran and E Ozbay, *Appl. Phys. Lett.* **77**, 3902 (2000)
[2] E D V Nagesh, G Santosh Babu, V Subramanian, V Sivasubramanian and V R K Murthy, *Pramana – J. Phys.* **65**, 11150 (2005)
[3] V Subramanian, *Pramana – J. Phys.* **70**, 739 (2008)
[4] H Rahimi, A Namdar, S Roshan Entezar and H Tajalli, *Pramana – J. Phys.* **74**, 805 (2010)
[5] K Sakoda, *Optical properties of photonic crystals* (Springer-Verlag, Berlin, 2001)
[6] K Inoue and K Ohtaka, *Photonic crystals: Physics fabrication and applications* (Springer, Berlin, 2004)
[7] M D Huang, S Y Park, Y P Lee and K W Kim, *J. Korean Phys. Soc.* **47**, 964 (2005)
[8] Y Kalra and R K Sinha, *Pramana – J. Phys.* **70**, 153 (2008)
[9] Y Liu and Z Lu, *Prog. Electromagn. Res.* **111**, 213 (2011)
[10] J Danckaert, K Fobelets, I Veretennicoff, G Vitrant and R Reinisch, *Phys. Rev. B* **44**, 8214 (1991)
[11] S Roshan Entezar, *Prog. Electromagn. Res. M*, **14**, 33 (2010)
[12] V M Agranovich, S A Kiselev and D L Mills, *Phys. Rev. B* **44**, 10917 (1991)
[13] R Wang, J Dong and D Y Xing, *Phys. Rev. E* **55**, 6301 (1997)
[14] E Lidorikis, K Busch, Q M Li, C T Chan and C M Soukoulis, *Phys. Rev. B* **56**, 15090 (1997)
[15] H Inouyea and Y Kanemitsu, *Appl. Phys. Lett.* **82**, 1155 (2003)
[16] J He and M Cada, *Appl. Phys. Lett.* **61**, 2150 (1992)
[17] C Lixue, D Xiaoxu, D Weiqiang, C Liangcai and L Shutian, *Opt. Commun.* **209**, 491 (2002)
[18] R Ozaki, T Matsui, M Ozaki and K Yoshino, *Appl. Phys. Lett.* **82**, 3593 (2003)
[19] R Ozaki, Y Matsuhisa, M Ozaki and K Yoshino, *Appl. Phys. Lett.* **84**, 1844 (2004)
[20] L Gao, J P Huang and K W Yu, *Phys. Rev. B* **69**, 075105 (2004)
[21] J P Huang and K W Yu, *Appl. Phys. Lett.* **85**, 94 (2004)
[22] J P Huang and K W Yu, *Opt. Lett.* **30**, 275 (2005)
[23] H P Chiang, P T Leung and W S Tse, *J. Phys. Chem. B* **104**, 2348 (2000)
[24] H T Jiang, H Chen, H Q Li, Y W Zhang and S Y Zhu, *Appl. Phys. Lett.* **83**, 5386 (2003)
[25] M Kohmoto, B Sutherland and K Iguchi, *Phys. Rev. Lett.* **58**, 2436 (1987)
[26] Z Wang, R W Peng, F Qiu, Z H Tang, X F Hu, X Q Huang *et al*, *J. Crystal Growth* **275**, e1209 (2005)
[27] S M Wang and L Gao, *Opt. Commun.* **267**, 197 (2006)
[28] C S Kee, J E Kim, H Y Park and H Lim, *IEEE Trans. Microw. Theory Tech.* **47**, 2148 (1999)
[29] Z F Sang and Z Y Li, *Opt. Commun.* **259**, 174 (2006)
[30] W Chen and D L Mills, *Phys. Rev. Lett.* **58**, 160 (1987)
[31] W Chen and D L Mills, *Phys. Rev. B* **36**, 6269 (1987)
[32] M Z Ali and T Abdullah, *Phys. Lett. A* **372**, 1695 (2008)
[33] Y Maeda, *Mater. Sci. Eng. B* **81**, 174 (2001)
[34] M Samoc, A Samoc, B Luther-Davies and M Woodruff, *Pure Appl. Opt.* **5**, 681 (1996)
[35] S Ohke, T Umeda and Y Cho, *Jpn. J. Appl. Phys.* **37**, L1312 (1998)